Infection with a Hypervirulent Strain of *Helicobacter Pylori* Primes Gastric Cells Toward Intestinal Transdifferentiation

Samaneh Saberi
HPGC Research Group, Department of Medical Biotechnology, Biotechnology Research Center, Pasteur Institute of Iran, Tehran

Maryam Esmaeili
HPGC Research Group, Department of Medical Biotechnology, Biotechnology Research Center, Pasteur Institute of Iran, Tehran

Mohammad Tashakoripour
Gastroenterology Department, Amiralam Hospital, Tehran University of Medical Sciences, Tehran

Mahmoud Eshagh Hosseini
Gastroenterology Department, Amiralam Hospital, Tehran University of Medical Sciences, Tehran

Hossein Baharvand
Department of Stem Cells and Developmental Biology at Cell Science Research Center, Royan Institute for Stem Cell Biology and Technology, ACECR, Tehran

Marjan Mohammadi (marjan.mohammadi2010@gmail.com)
HPGC Research Group, Department of Medical Biotechnology, Biotechnology Research Center, Pasteur Institute of Iran, Tehran

---

Research Article

Keywords: Helicobacter pylori, Wnt signalling, intestinal metaplasia, gastric cancer, transdifferentiation.

Posted Date: September 14th, 2021

DOI: https://doi.org/10.21203/rs.3.rs-866653/v1

Version of Record: A version of this preprint was published at Microbial Pathogenesis on December 1st, 2021. See the published version at https://doi.org/10.1016/j.micpath.2021.105353.

Abstract

Background: Intestinal metaplasia, gastric-to-intestinal transdifferentiation, occurs as a result of the misexpression of certain regulatory factors, leading to genetic reprogramming. Here, we have evaluated the *H. pylori*-induced expression patterns of these candidate genes.

Methods: The expression levels of 1)tissue-specific transcription factors (*RUNX3, KLF5, SOX2, SALL4, CDX1 and CDX*2), 2)stemness factors (*TNFRSF19, LGR5, VIL1*) and 3)tissue-specific mucins (*MUC5AC, MUC2*) were evaluated by quantitative real-time PCR in gastric primary cells (GPCs), in parallel with two gastric cancer (MKN45 and AGS) cell lines, up to 96h following *H. pylori* infection.

Results: Following *H. pylori* infection of GPCs, *RUNX3* declined at 24h post infection (PI) (-6.2±0.3) and remained downregulated for up to 96h. Subsequently, overexpression of self-renewal and pluripotency transcription factors, *KLF5* (3.6±0.2), *SOX2* (7.6±0.5) and *SALL4* (4.3±0.2) occurred. The expression of *TNFRSF19* and *LGR5*, demonstrated opposing trends, with an early rise of the former (4.5±0.3) at 8h, and a simultaneous fall of the latter (-1.8±0.5). This trend was reversed at 96h, with the decline in *TNFRSF19* (-5.5±0.2), and escalation of *LGR5* (2.6±0.2) and *VIL1* (1.8±0.3). Ultimately, *CDX1* and *CDX2* were upregulated by 1.9 and 4.7-fold, respectively. The above scenario was, variably observed in MKN45 and AGS cells.

Conclusion: Our data suggests an interdependent gene regulatory network, induced by *H. pylori* infection. This interaction begins with the downregulation of *RUNX3*, upregulation of self-renewal and pluripotency transcription factors, *KLF5*, *SOX2* and *SALL4*, leading to the downregulation of *TNFRSF19*, upregulation of *LGR5* and aberrant expression of intestine-specific transcription factors, potentially facilitating the process of gastric-to-intestinal transdifferentiation.

1. Introduction

Helicobacter pylori infects the majority of the population in the developing world [1]. This infection induces a number of complications, ranging from chronic active gastritis to peptic ulcers and gastric cancer (GC) [2,3]. Gastric cancer is the fourth most common cancer worldwide and ranks as the second leading cause of cancer-related deaths [4]. Histologically, according to Lauren's classification, intestinal type gastric cancer is one of the major subtypes of gastric adenocarcinoma with precancerous processes, clinical features and epidemiology, different from the diffuse subtype [5,6]. Intestinal type GC develops from a multi-step alteration process, which begins with superficial gastritis and can progress to chronic and then atrophic gastritis, leading to intestinal metaplasia (IM) and ultimately intestinal type GC [7]. Accordingly, the annual incidence of GC, within the five years post diagnosis, is 2.5-fold higher in those with IM [8].

The gastric-to-intestine metaplasia is a postnatal 'transdifferentiation" process, in which terminally differentiated gastric cells, are irreversibly replaced by adult intestinal cells [9]. Both the stomach and the intestine originate from the same endodermal lineage in the early embryo [10], and their fate is decided by a

gradient of induction factors and specific gene signatures for each tissue [11]. Normally, “master control genes” encoding transcription factors, control this development rather than a multitude of genes [12]. During gastric-to-intestinal transdifferentiation, a major alteration in gene expression, especially of tissue-specific transcription factors, result in switching off one set of downstream genes and switching on another [13].

On the other hands, there is a worldwide correlation between *H. pylori* infection and the incidence of GC, mostly of the intestinal subtype [14]. Several pathways are involved in gastric carcinogenesis, amongst which the Wnt signalling pathway plays a fundamental role [15]. This pathway is a critical regulator of the gastrointestinal development and maintenance, employing multiple arrays of molecules, which interact to adjust, activate or suppress different subsets of transcription factors, leading to stem cell identities and various differentiation fates [15]. In other words, the Wnt signalling pathway maintains the homeostasis of the normal gastric epithelium by balancing stem cell maintenance and proliferation, the dysregulation of which plays a critical role in the development of more than 30% of gastric tumors and also observed in gastric cancer cell lines [16–18]. Numerous genes such as *KLF5, TNFRSF19, LGR5, CDX1* and *CDX2* are affected by the canonical Wnt signalling pathway [19]. *H. pylori* is, indeed, a major disruptive factor in this pathway [20]. Notably, *H. pylori*, *via* the Wnt/β-catenin pathway, induces gastric stem cell generation and expansion, promoting gastric cancer initiation and progression. Through its oncogenic protein, CagA, *H. pylori* can induce aberrations in stemness gene expression, particularly leucine-rich repeat-containing G-protein coupled receptor (LGR)5-positive stem cell proliferation [21]. Conversely, the expression of a member of the tumor necrosis factor receptor superfamily called TNFRSF19 [19], is believed to function as a negative modulator of the Wnt pathway, in particular on LGR5-positive stem cells [19]. Another inhibitory molecule on this pathway is RUNX3, which is also modulated by *H. pylori* infection [22]. Moreover, *SOX2* is one of the key transcription factors in the foregut region known to promote stemness by upregulating genes involved in self-renewal and pluripotency, and suppressing those involved in the development of mature differentiated cells [23]. It has been reported that SOX2 is also overexpressed in cancer stem cells (CSCs) [23]. Finally, once the process of gastric IM occurs, the type of cell surface mucins will be altered to match the substituted (intestinal) tissue. Mucins are heavily glycosylated glycoproteins which constitute the major components of the protective mucous gel covering the surface epithelial tissues [24]. Immunohistology staining of the normal gastric mucosa shows cell type-specific expression of MUC1, MUC5AC, and MUC6, with first two mucins found in the superficial epithelium and MUC6 in the deep glands [25]. MUC2 is the main mucin of the intestinal mucosa [26], and fully absent in the normal gastric epithelium [27].

The goal of this study was to assess the regulation of the above-mentioned cascade of gene signatures during the course of time, following *H. pylori* infection of gastric primary cells (GPCs), as compared to two gastric cancer (MKN45 and AGS) cell lines. For this purpose, the three categories of tissue-specific transcription factors (*RUNX3, KLF5, SOX2, SALL4, CDX1* and *CDX2*), the stemness markers (*TNFRSF19, LGR5 and VIL1*) and tissue-specific mucins (*MUC5AC and MUC2*) were traced over time post infection.

2. Results

2.1. Baseline gene expression patterns over time

We, primarily, compared baseline expression of our target genes in two gastric primary cells from two different donors (GPCs1 and GPCs2), at two different time points (1st and 3rd months). The gene signatures of both cells remained consistent over time and were located in the same cluster as the normal gastric tissue. [Euclidean distances, (GPCs1:1st month: 15.4 and 3rd month: 15.1) and (GPCs2: 1st month: 17.3 and 3rd month: 17.2)] and apart from the duodenum or Tumor [Euclidean distances, (GPCs1:1st month: 20.5 and 3rd month: 20.8) and (GPCs2: 1st month: 23.7 and 3rd month: 23.1)]. Therefore, GPCs1 was selected for further studies and was referred to as GPCs, throughout the study (Supplementary Fig. 1). Next, we assessed baseline expression of the target genes in GPCs, MKN45, and AGS cells up to 96 h of culture. Accordingly, the baseline mRNA levels and relative gene expression for the three groups of 1) tissue-specific transcription factors (*RUNX3, KLF5, SOX2, SALL4, CDX1 and CDX2*), 2) stemness factors (*TNFRSF19, LGR5, VIL1*) and 3) tissue-specific mucins (*MUC5AC, MUC2*) were found to be consistent over time (Fig. 1A). According to their comparative gene expression profiles, the three cell lines behaved as follows: Of the first category of genes, *SOX2*, *SALL4*, and *CDX1* were similarly expressed amongst the three cell lines. Whereas, *RUNX3* and *KLF5* were produced at lower and higher levels in AGS and GPCs, respectively (Fig. 1A). The levels of *CDX2* expression were observed in the following sequence: AGS > MKN45 > GPCs. Of the second category of genes, GPCs and AGS cells were *TNFRSF19* and *VIL1* -high and -low producers, respectively and *LGR5* was equally expressed amongst the three cell lines (Fig. 1A). In the category of mucins, GPCs were high producers, particularly of *MUC5AC*, followed by MKN45 and AGS cells, respectively (Fig. 1A).

A heatmap was depicted in order to classify the cells according to the proximity of their baseline gene expression profiles to the gastric *versus* intestinal origins (Fig. 1B). As a result, GPCs appeared closer to the normal gastric tissue (Euclidean distance of 3.82) and apart from the other two (AGS and MKN45) cells, as well as the tumor tissue (Euclidean distance of 8.22). Whereas, AGS and MKN45 cells appeared closer together (Euclidean distance of 1.09) and in the vicinity of the intestinal type tumor (Euclidean distance of 1.76), followed by the duodenal tissue. Therefore, due to their gastric nature, the GPCs were selected as the primary model system for assessment of time-dependent gene expression, following *H. pylori* infection, against which the corresponding profiles of the MKN45 and AGS cancer cell lines were compared.

2.2. Characterization of the hypervirulent *H. pylori* strain

The selected hypervirulent strain of *H. pylori* (C142LD) strain for cell culture infections, was identified as a gram-negative, helically-shaped, urease, catalase, and oxidase-positive bacterium, which was positive for *H. pylori ureC* (*glmM*) gene (Fig. 2A). Its *cagA*, *vacA* and *babA* genotypes were determined as *cagA*-positive (ABCCC-type), *vacA s1m1i1* and *babA* AA type, respectively (Fig. 2A). This strain expressed the CagA/VacA/BabA gene products (Fig. 2B) and was able to induce cellular vacuolation and the

hummingbird phenotype as early as 24h PI, which intensified at 48h PI (Fig. 2C). Therefore, the C142LD strain was considered as hypervirulent [28].

2.3. Characterization of *H. pylori* coculture

During the co-culture assay, the interactions between the hypervirulent *H. pylori* strain and gastric cells, were investigated by the following assays: 1) induction of morphologic changes: vacuolation and hummingbird phenotypes were detected in GPCs, as well as AGS, and MKN45 cells (Supplementary Fig. 2A), at 24h PI, 2) the effect of *H. pylori* infection on cell viability was examined during the entire assay (0-96h). Accordingly, in all three cells, the OD_{450} increased over time, which was a sign of cells growing during the course of the experiment (Supplementary Fig. 2B), 3). At 24h PI, IL-8 production was detected in GPCs (529.8 ± 5.4 pg/10^6 cells) [29], MKN45 (883.5 ± 12.7 pg/10^6 cells) and AGS (302.2 ± 9.7 pg/10^6 cells), as compared to uninfected controls ($P < 0.0001$, Supplementary Fig. 2C).

2.4. Gene signatures following *H. pylori* infection

The expression patterns of our three categories of target genes (tissue-specific transcription factors, stemness markers and tissue-specific mucins), suspected to be involved in the process of gastric-to-intestinal transdifferentiation were then assessed, in GPCs, as the primary model, against which the corresponding profiles of two gastric cancer (MKN45 and AGS) cell lines were compared, up to 96h following *H. pylori* infection.

2.4.1. Tissue-specific transcription factors

H. pylori infection of GPCs, resulted in an early reduction in *RUNX3* and a significant escalation of *KLF5, SOX2* and *SALL4* genes expression, in reference to untreated cells (Fig. 3). In other words, following a sudden peak at 8h PI (2.9 ± 0.3, $P < 0.0001$), the expression level of *RUNX3* declined by more than 7 times (-6.2 ± 0.3, $P < 0.0001$), at 24h PI and despite an increasing trend in 48h (-1.9 ± 0.3, $P < 0.0001$) to 96h (-0.8 ± 0.5, $P < 0.0001$), as compared to 24h PI, it remained significantly downregulated, throughout the experiment as compared to uninfected cells (Fig. 3A). In contrast, the expression levels of *KLF5* increased and peaked at 8h PI hours (3.6 ± 0.2, $P < 0.0001$), followed by *SOX2* (7.6 ± 0.5, $P < 0.0001$) and *SALL4* (4.3 ± 0.2, $P < 0.0001$) at 24h PI, all of which remained elevated for up to 96h, in reference to untreated cells (Fig. 3B-D). In parallel, a small peak of *CDX1* expression was detected at 8h PI (2.0 ± 0.4, $P < 0.0001$), which dropped to baseline, at 24h and remained there until another slight rise at 96h PI (1.9 ± 0.1, $P = 0.004$, Fig. 3E). Alongside *CDX1, CDX2* gene expression developed a rising trend, at 48h PI (2.5 ± 0.3, $P < 0.0001$) and reached nearly 5 fold upregulation, at 96h (4.7 ± 0.1, $P < 0.0001$), as compared to the uninfected cells (Fig. 3F).

The expression pattern of *RUNX3* in *H. pylori*-infected MKN45 cells similar to GPCs, demonstrated a decrease, but at a much smaller scale (Fig. 3A). It, then, returned to near baseline expression at 48-96h PI (Fig. 3A). Very similar to the pattern of *KLF5* expression in GPCs, that of MKN45 also had a rising trend, with an initial peak at 8h, followed by a steady state of expression at 24h to 96h PI (Fig. 3B). The same

occurred for *SOX2* expression, with an early peak at 8h, which was nearly double that of GPCs, at that time point. But then, declined at 24h. Nevertheless, it remained upregulated up to 96h PI (Fig. 3C). This increasing pattern was also observed for *SALL4* expression in *H. pylori*-infected MKN45 cells, as compared to uninfected cells, throughout the experiment. However, initially there was an upward trend similar to GPCs, but then unlike GPCs, it took a downward trend (Fig. 3D). In terms of the intestinal transcription factors, the expression of *CDX1* in MKN45 was highly upregulated, compared to uninfected cells, throughout the experiment and maintained a rising trend (Fig. 3E). The expression of *CDX2* in these cells was also upregulated (but to a lesser degree than *CDX1*), as compared to uninfected cells throughout the experiment (Fig. 3F). Except for the initial peaks, the observed rising trend was quite similar to that of GPCs.

The expression of *RUNX3* in *H. pylori*-infected AGS cells, unlike GPCs, declined early post infection, and returned to near baseline expression at 48 -96h (Fig. 3A). Very similar to the pattern of *KLF5* expression in GPCs and MKN45 cells, that of AGS cells also had a rising trend, with an initial peak at 8h, followed by a steady state overexpression at 24h to 96h PI (Fig. 3B). The expression of *SOX2* in AGS cells, was upregulated, compared to uninfected cells, throughout the experiment but, unlike GPCs, had an overall reducing trend. A 1.5 times initial overexpression of *SOX2*, compared to that of GPCs, at 8h PI, was observed, followed by a decreasing trend at 24-96h PI (Fig. 3C). The same occurred for *SALL4* expression, with an early peak at 8-24h PI, which was 1–4 times that of GPCs. But then, declined at 48-96h PI (Fig. 3D). The expression of the intestinal transcription factors, *CDX1*, in AGS had an early fall and a late peak, which was almost double that of GPCs, at 96h PI (Fig. 3E). The expression of *CDX2*, however, in AGS cells had a rising trend, throughout the experiment, which nearly coincided with that of GPCs at 48-96h PI (Fig. 3F).

2.4.2. Stemness markers

In GPCs, the expression of the stemness markers, in particular *TNFRSF19* and *LGR5*, demonstrated an opposing trend, during the time course of *H. pylori* infection (Fig. 3G-H). In other words, the former depicted an early rise (4.5 ± 0.3, $P < 0.0001$, Fig. 3G) at 8h PI, coinciding with a simultaneous fall of the latter (-1.8 ± 0.5 at 8h, $P < 0.0001$, down to -11.1 ± 0.7 at 24h, $P < 0.0001$, Fig. 3H). Whereas, this trend was reversed at the latest time point (96h PI), such that the decline in *TNFRSF19* (-5.5 ± 0.2, $P < 0.0001$, Fig. 3G) coincided with the escalation of *LGR5* (2.6 ± 0.2, $P < 0.0001$, Fig. 3H). Throughout this time, expression of *VIL1* experienced two separate peaks at 24h (2.7 ± 0.2, $P < 0.0001$) and 72h (2.4 ± 0.4, $P < 0.0001$), as compared to the untreated cells (Fig. 3I).

The expression of *TNFRSF19* in *H. pylori*-infected MKN45 cells, similar to that of GPCs, was biphasic, with an early peak and a late drop, as compared to uninfected cells (Fig. 3G-H). *LGR5* expression, however, was mostly up-regulated, with two peaks at 8h and 72-96h PI (Fig. 3H). Similar to GPCs, however, the final peak in *LGR5* in MKN45 cells at 96h PI, coincided with the down-regulation of *TNFRSF19* (Fig. 3G-H). The expression of *VIL1* in MKN45 cells, on the other hand, contrasted with its early peak in GPCs, though coinciding with the late peak at 96h PI (Fig. 3I).

TNFRSF19 expression in *H. pylori*-infected AGS cells was upregulated, as compared to uninfected cells throughout the experiment, which was similar to that of GPCs, but with lower extent, up to 72h PI, after which unlike that of GPCs, it remained upregulated up to 96h (Fig. 3G). *LGR5* expression, in AGS cells, in contrast to that of GPCs, was upregulated at the beginning, but returned to baseline by the 96h (Fig. 3H). The expression of *VIL1* in AGS cells, also remained upregulated throughout the experiment, which was similar to that of GPCs, at 24 and 72h PI (Fig. 3I).

2.4.3. Tissue-specific mucins

The expression patterns of gastric-specific (*MUC5AC*) and intestine-specific (*MUC2*) mucins of *H. pylori*-infected GPCs are illustrated in Fig. 3J-K, which indicate a significant peak for *MUC5AC* expression, following 24h PI (2.9 ± 0.2, $P < 0.0001$), which declined by the end (at 96h, 1.4 ± 0.2, $P = 0.5$, Fig. 3J). This coincided with a sharp decline in *MUC2* (-5.2 ± 0.2 at 8h PI), which picked up at 96h (-0.3 ± 0.5, $P < 0.0001$, Fig. 3K) post infection, though remained below baseline.

The expression of *MUC5AC*, in *H. pylori*-infected MKN45 cells, was very similar to that of GPCs. Such that it was up-regulated throughout the experiment, although with a much higher intensity than in GPCs (Fig. 3J). *MUC2* expression in MKN45 cells, however behaved the exact opposite of GPCs, with the upregulation in the former *versus* down-regulation in the latter cell line (Fig. 3K).

The expression of *MUC5AC* in *H. pylori*-infected AGS cells, similar to that of GPCs, had an early rise at 8h PI, but underwent a drastic fall at 48h, which picked up again at 72-96h PI, but remained below baseline (Fig. 3J). As for *MUC2* expression in AGS cells, it followed the same direction as that of GPCs, except that it crossed the baseline at 48h PI, and remained overexpressed up to 96h PI (Fig. 3K).

2.5. Time-course of gene expression

In order to better understand the patterns and trends of gene expression following *H. pylori* infection in each cell line, we defined gene expression patterns, as “altered” if variations occurred at > 100% higher or lower, than that of the uninfected cells, as presented in the collective gene signatures of each cell line, during early (0–24 h) and late (24-96h) stages post infection (Fig. 4). Amongst, tissue-specific transcription factors, the expression of *RUNX3*, was consistently and strongly downregulated in GPCs (Fig. 4A). But in MKN45 and AGS cells, its underexpression occurred, only early after infection, with lesser intensity in both cancer cell lines (Fig. 4B-C). In contrast, *KLF5, SOX2* and *SALL4* were consistently upregulated in all three cell lines, throughout the experiment (Fig. 4A-C). As for intestinal type transcription factors, *CDX1* was strongly upregulated in MKN45 (early and late, Fig. 4B) and AGS (late, Fig. 4C) cell lines and to a much lesser degree in GPCs (early, Fig. 4A) post infection. *CDX2* however, was strongly over-expressed, in all 3 cell lines, late post infection (Fig. 4A-C). In the stemness marker group, *TNFRSF19* was first upregulated in GPCs and MKN45, then down regulated (Fig. 4A-B). This coincided with an opposite trend for *LGR5* in GPCs (throughout, Fig. 4A) and late after infection for MKN45 cells (Fig. 4B). However, these two stemness factors (*TNFRSF19* and *LGR5*) were both upregulated in AGS cells, albeit still an alternating sequence (Fig. 4C). As for *VIL1*, it was mostly upregulated in GPCs and AGS cells (Fig. 4A & C). But in MKN45 cells, it was initially downregulated, then upregulated (Fig. 4B).

Regarding tissue-specific mucins, the expression of *MUC5AC* and *MUC2* had opposing trends in GPCs and AGS cells, although in reverse order. Whereas, they were both extensively upregulated in MKN45 cells (Fig. 4A-C).

2.6. Comparative gene expression signatures in gastric primary cells (GPCs) vs. cancerous cell lines (MKN45 and AGS)

The above-stated results indicate similarities and differences, in their pattern of gene expression, following *H. pylori* infection, amongst gastric primary cells, as our model system, in reference to gastric cancer cell lines. The results of the heatmap and correlation clustering showed that GPCs' gene expression signature starts near the profile of normal gastric tissue early (8-24h) after infection, and moves toward that of the intestinal type tumor tissue, late after *H. pylori* infection (Fig. 5A). As a result, GPCs at 48-96h PI appeared closer to the intestinal type tumor (Euclidean distances: 11.7, 14.2 and 12.1) and apart from the normal gastric tissue (Euclidean distances: 19.5, 21.5 and 22.8). On the other hand, MKN45 (Euclidean distance: 14.1, 12.1, 11.3, 11.5 and 12.3) and AGS (Euclidean distances: 9.9, 9.9, 9.7, 10.4 and 12.7) cells, at both early (8-24h PI) and late (48-96h PI) stages post infection, remained as united clusters and in the vicinity of intestinal type gastric tumor (Fig. 5B-C).

3. Discussion

The hypothesis of this study was that in the process of gastric-to-intestinal transdifferentiation, due to *H. pylori* infection, a terminally differentiated gastric cell undergoes a reduction in gastric-specific and an escalation in progenitor/intestine-specific factors, respectively.

H. pylori infection, in the harsh acidic milieu of the stomach, induces a cascade of pathologic changes, to which a series of virulence factors contribute [28,30]. These predominantly include CagA [31–33], VacA [34] and BabA adhesin [35,36]. Such that patients infected with *cagA+, s1m1, babA2 + H. pylori*, are at more than 23 fold increased risk of severe gastrointestinal complication, as compared to *cagA-, s2m2, babA2-* strains [30], and the risk of gastric cancer in the former group is 6.4 times higher than that in the latter [28]. In our study, we have used a *cagA*+ (ABCCC-type), *vacA* s1m1i1 and *babA* AA, hypervirulent *H. pylori* strain, which was also capable of inducing cellular elongation and vacuolation, as well as IL-8 production. This hypervirulent strain was co-cultured with gastric primary cells (GPCs) and two commonly used (MKN45 and AGS) cancer cell lines, for 8, 24, 48, 72, and 96 hours and the expression profiles of the following 3 categories of genes were assessed: 1) tissue-specific transcription factors (*RUNX3, KLF5, SOX2, SALL4, CDX1 and CDX*2), 2) stemness factors (*TNFRSF19, LGR5, VIL1*) and 3) tissue-specific mucins (*MUC5AC, MUC2*).

First and foremost, to understand the essence of the studied cells, we examined their gene expression and clustered them by drawing gene expression charts and heat maps. Of these cells, the non-transformed (non-cancerous) primary cells (GPCs [29]) clustered with the normal gastric tissue. Whereas, the essence of MKN45 and AGS cells was closer together and clustered with the intestinal type gastric tumor and duodenal tissue. In recent years, several attempts have been made to elegantly build a suitable model for *in vitro* infection of *H. pylori*, ranging from one-dimensional gastric cancer cell lines [37] to three-dimensional, patient-derived organoids [38]. The former group include MKN45 [39] and AGS [40] cancer cell lines, which are already transformed, as manifested by their prominent expression of intestine-specific genes, *i.e. CDX2*, *MUC2*, *TFF3* [41], *Vll1*, *LGALS4* and *LI-cadherin* [42]. By definition, these cancer cell lines have already undergone gastric-to-intestinal transdifferentiation (transformation), evidenced by the down regulation of *p53* gene, *CDK2* and *G1* cyclins expression, homozygous deletion of the *p16* and *p15* genes or *p27* gene rearrangement, promoter mutation of E-cadherin, etc. [42,43]. According to these reports and in line with our results, gene expression patterns of these cancerous cell lines (MKN45 and AGS) are closer to the intestinal type tumor and the duodenum, rather than the normal stomach [42]. Therefore, assessing alteration in gene expression patterns, subsequent to *H. pylori* infection in gastric primary cells (GPCs), relative to these cell lines, may provide a more realistic insight.

Based on the behaviour of GPCs, the obtained data suggest an interdependent gene regulatory network, induced by *H. pylori* infection. This interaction begins with the downregulation of *RUNX3*, upregulation of self-renewal and pluripotency transcription factors, *KLF5*, *SOX2* and *SALL4*, leading to the downregulation of *TNFRSF19* and upregulation of *LGR5* and aberrant expression of intestine-specific transcription factors, particularly *CDX2*, thereby facilitating the process of gastric-to-intestinal transdifferentiation.

This network of interactions is activated by *H. pylori* infection, which affects the Wnt pathway in three aspects. It primarily lifts the inhibitory role of RUNX3, by causing its gene hypermethylation (inactivation) and mislocation [44]. Secondly, it disrupts the E-cadhein/β-catenin interaction between epithelial cells, by injecting CagA oncoprotein into the cells and causing excessive accumulation of β-catenin in the cytoplasm, part of which enters the nucleus [45] and transcribes the Wnt responsive genes, such as cell cycle control, pluripotent [46], and self-renewal genes of cancer and stem cells [47] and ultimately, aberrant expression of *CDX1* and *CDX2* and occurrence of intestinal metaplasia [48]. Since, we have, herein, used a hypervirulent strain of *H. pylori*, the reduction in *RUNX3* gene expression in GPCs was clearly observed. This phenomenon was also observed in MKN45 and AGS cancer cell lines, but with less intensity coinciding with or earlier than GPCs, respectively, which returned to baseline expression at late time points. This observation may be due to the earlier onset of *RUNX3* down regulation in these two cells, as they have already experienced this process in their previous malignant transformation, as evidenced by the cytoplasmic localization of *RUNX3* in MKN45 [49] and its inactivation in AGS [50].

A recent study on 192 GC patients, whose tumor tissues were analysed by methylation-specific PCR and IHC, demonstrated significant *RUNX3* promoter hypermethylation (40.6%, 78/192) and subsequent protein underexpression (51.65%, 99/192) [51]. This pattern was found closely associated with *H. pylori*

infection [51]. In addition, a study of 154 healthy volunteers revealed that *RUNX3* CpG island methylation was significantly higher (5.4 to 303-fold) in *H. pylori*-positive *versus* negative subjects [52]. On the other hand, several meta-analyses have confirmed the close association between *RUNX3* gene downregulation and gastric cancer development [53–55] and disease progression [56]. How *H. pylori* manages to downregulate *RUNX3* gene expression may be due to its indirect activation of DNA methyltransferases *via* inflammatory mediators [57], and/or the direct effect of CagA [57]. Nevertheless, when *RUNX3* is downregulated, its inhibitory role is lifted and aberrant activation of the Wnt signalling pathway, leading to spontaneous epithelial-mesenchymal transition (EMT) and production of tumorigenic stem cell-like subpopulations, occurs [58]. In line with this scenario, we observed *SOX2*, *SALL4* and *KLF5*, upregulation, at early time points, which mostly remained as such, in the other two cell lines, albeit to a lesser extent, throughout the experiment.

SOX2 expression plays an important role in regulating tissue development and cell differentiation, as this factor is highly expressed in the foregut region, during embryonic development, giving rise to the stomach and generating the boundary between the posterior stomach and the proximal intestine [59]. Generated Sox2-GFP indicator mice from embryonic stem cells (ESCs) reveal that, in adulthood, SOX2 + cells are located in the base of the pyloric and corpus glands, capable of generating surface mucous, chief, parietal, and enteroendocrine cells of the gastric units [60], ablation of which results in the disruption of the physiological renewal of the gastric epithelium [60]. The role of SOX2, in gastric cancer development, however, remains obscure. Studies can be categorized in three groups, as those having provided evidence in support of [61–65] or against [65,66] its role in gastric carcinogenesis, as well as those which have found no significant association [67]. In particular, analysing normal gastric mucosae, intestinal metaplasia and tumor tissues of 68 gastric carcinoma patients by IHC, showed SOX2 as moderately expressed in sites with intestinal metaplasia [62]. In the gastric tumors, however, SOX2 is mainly expressed at sites with high proliferation rates [68]. Therefore, SOX2 is considered functionally active in cancer stem cells, maintaining their self-renewal capacity [68]. Considering these results, the elevated expression of *SOX2* in GPCs, may primarily be due to the formation of a subpopulation of progenitor cells, further supported by the simultaneous/subsequent upregulation of *SALL4* and *KLF5* expression. *SALL4* [69] and *KLF5* [70] are considered as oncogenes and distinguished as stemness-related reprogramming factors. SALL4 is aberrantly expressed through the Wnt/β-catenin pathway in several human malignancies, such as oesophageal squamous cell carcinoma [71], osteosarcoma[72], leukaemia [73], and gastric cancer [74]. Its expression is closely correlated with a poor outcome and resistance to therapy [71]. SALL4 expression in the normal stomach is limited to the proliferating and stem cells areas, though its expression in gastric tumor tissues is also detected [75]. Likewise, the expression of *KLF5* increases in the process of gastric carcinogenesis, and is particularly detected in tissues with intestinal metaplasia and dysplasia [76]. This transcription factor is critical in maintaining the integrity of intestinal stem-cells [77]. Expression of these two stemness-related reprogramming factors indicates the emergence of a subpopulation of progenitor cells, which may play an intermediary role in the gastric-to-intestinal transdifferentiation process. *H. pylori* infected MKN45 and AGS cancer cell lines also showed initial *KLF5*, *SOX2* and *SALL4* overexpression,

which remained elevated throughout the experiment, respectively. Studies show that MKN45 and AGS cells contain large populations of cancer stem cells capable of spheroid and tumor formation *in vitro* and *in vivo* [78,79]. Thus, their initial higher expression of *KLF5*, *SOX2* and *SALL4* may be due to the presence of larger starting population of cancer stem cells in MKN45 and AGS cells, prior to infection.

On a different note, using immunohistochemistry, we have previously reported an inverse trend between *TNFRS19* downregulation and *LGR5* upregulation in gastric cancer tumours in humans, as well as in response to *H. pylori* infection in mice [80]. Other studies also support a potential negative modulatory role for *TNFRSF19* on *LGR5* expression [19] and the Wnt signalling pathway [81]. For instance, *TNFRSF19* overexpression in MKN45 cells, leads to their decreased clonal expansion [81]. LGR5 is a stem cell surface receptor and gastric LGR5 + cells have a structure similar to the undifferentiated stem cell population, with large nuclei, limited rough endoplasmic reticula and absence of secretory granules [46]. *H. pylori* is known to affect gastric precursor cells, leading to increased proliferation and expression of LGR5 + cells [21], which is higher prevalent in the gastric tumor than the non-cancerous surrounding tissues, as a marker of dedifferentiation [82]. Furthermore, it has been revealed that LGR5 is considered as a marker of intestinal stem cells [83], and its overexpression at the end of our experiment may due to the appearance of an intestinal progenitor subpopulation. We have, herein, observed that a reduction in *TNFRSF19* coincided with the escalation of *LGR5*, at the latest time point in GPCs. A similar pattern was also observed for *H. pylori*-infected MKN45 cells. This inverse trend between *TNFRSF19* and *LGR5*, was also slightly observed in the consistently upregulated AGS cells. In regards to the development of intestinal progenitor subpopulations, Villin, which is the building block of the intestinal microvilli [84] and has also been designated as an indicator of dormant gastric stem cells [85], is also under focus. Our result showed that *VIL1* gene expression experienced late peaks, in all three cell lines, which further conforms with this concept.

Finally, in the gastric to intestinal transdifferentiation process, it is ultimately expected that the intestine-specific transcription factors undergo upregulation. Accordingly, we observed that both *CDX1* and *CDX2*, had an increasing trend in GPCs, as well as MKN45 and AGS, but with varying patterns. The expression of *CDX1* peaked but declined in GPCs, early and late after infection, respectively. Whereas, in MKN45 cells this rise began early and persisted up to late stages, when, AGS cells joined in. The Caudal homeobox gene family is responsible for differentiating the endoderm into the posterior endoderm and are distinguished as intestine-specific transcription factors [86]. The activities of the two *CDX1* and *CDX2* transcription factors are limited to the middle and posterior intestinal region [87] and both are essential in the regulation of the intestinal cell proliferation and differentiation [88]. It has also been shown that the undifferentiated cells of the intestinal crypts express *CDX1* predominantly, whereas the differentiated cell of intestinal villi, mostly express *CDX2* [88]. On the other hand, the aberrant expression of CDX1 is detected in areas of the stomach and oesophagus affected by intestinal metaplasia [89]. Studies have shown that the Wnt signalling pathway regulates both *CDX1* [90] and *CDX2* [91] and that *H. pylori* increases their expression [92,93]. Given these findings and the results obtained herein, it seems that following infection

with a hypervirulent strain of *H. pylori* and activation of the Wnt pathway, the progenitor subpopulations initiate the gastric-to-intestinal transdifferentiation process, by aberrant expression of *CDX1* and *CDX2*. In GPCs, with normal gastric nature, undifferentiated intestinal subpopulations expressing *CDX1* and differentiated intestinal subpopulation expressing *CDX2*, appeared at early and then late time points, respectively. Whereas in MKN and AGS ells, with cancerous and mostly intestinal nature, a mixture of *CDX1* expressing undifferentiated and *CDX2* expressing differentiated cells are formed earlier or at the final stages, respectively.

According to our hypothesis, the above interdependent network of gene expression would supposedly translate into downregulation of gastric-specific (MUC5AC) and upregulation of intestine-specific (MUC2) mucins. However, in GPCs, we observed a consistent upregulation of the former and downregulation (yet with a rising trend) of the latter. In MKN45 cells, both *MUC5AC* and *MUC2* were upregulated throughout the experiment. In AGS cells, an opposing trend was observed in the expression of these two tissue-specific mucins. As the colonization of Le^b-binding *H. pylori* strains, including our herein used hypervirulent strain, is dependent on MUC5AC [94], the upregulation of this receptor upon infection may be induced for better colonization. It is also hypothesized that, injection of CagA into gastric epithelial cells triggers an array of molecular cascades [95] leading to transient escalation in *MUC5AC* expression [96]. Accordingly, we observed an initial peak in *MUC5AC* expression, in all three cell lines. AGS cells, however, was the only cell line in which the previously expected pattern occurred, namely *MUC5AC* downregulation coincided with *MUC2* upregulation. In support of the observed pattern in AGS cells, a meta-analysis of 7 case-control studies (1997–2012) concluded that the presence of *H. pylori* decreases gastric epithelial expression of *MUC5AC*, by more than half [97] and its eradication restores its levels to some degree [98]. MUC5AC downregulation was also evident in gastric preneoplastic lesions, including areas with atrophic gastritis, intestinal metaplasia [27,99] and dysplasia [99]. As for MUC2, immunohistochemical and RNA northern and slot-blot analysis of normal and neoplastic human tissues confirmed its lack of expression in normal gastric epithelium, thereby restricting it to the intestines [100]. Consequently, the level of MUC2 is substantially increased, in intestinal metaplasia and intestinal type gastric cancer [27], particularly following *H. pylori* infection [101]. Histopathological and histochemical studies have divided intestinal metaplasia into two types: 1) complete or type I, which is characterized by the presence of absorptive, Paneth, and goblet cells and corresponds to the small intestine phenotype and 2) incomplete or types II and III, which are characterized by the presence of columnar and goblet cells [102]. It has been shown that in type I intestinal metaplasia “gastric” mucins (MUC1, MUC5AC, and MUC6) are decreased, while MUC2 is aberrantly expressed. In contrast in types II and III intestinal metaplasia, “gastric mucins” (MUC1, MUC5AC, and MUC6) are co-expressed with “intestinal” mucin (MUC2) [103]. Hence, our results may suggest that following *H. pylori* infection of MKN45 cells, the upregulation of both *MUC5AC* and *MUC2* may represent incomplete or types II/ III of intestinal metaplasia cells, in which copresence of intestinal differentiated cells, columnar and goblet cells, are expected. In contract in AGS cells, the inverse trend of *MUC5AC/MUC2* expression, may be due to the formation of complete or type I intestinal metaplasia.

In summary, GPCs as a non-cancerous primary cell culture model for *H. pylori* infection [29] seems to undergo transdifferentiation by downregulating *RUNX3* and *TNFRSF19*, up-regulating self-renewal and pluripotency transcription factors (*SOX2, KLF5* and *SALL4*), which then lead to the up-regulation of *LGR5* and aberrant expression of intestine-specific transcription factor, particularly *CDX2*. Aberrant expression of *MUC2* did not occur in these cells, during the time course of our experiment and might appear in prolonged cocultures. In contract, MKN45 and AGS cancerous cells, infected with *H. pylori* may manifest the process of transdifferentiation by upregulation of self-renewal and pluripotency transcription factors, due to their prior downregulation of *RUNX3*. In both cancer cell lines, the upregulation of *LGR5* and aberrant expression of *CDX2* is observed. However, in MKN45 cells, the simultaneous upregulation of *MUC5AC* and *MUC2* may represent incomplete types (II and III) intestinal metaplasia, whereas in AGS cells, their inverse trend may manifest the appearance of the complete type (I). In other words, upon *H. pylori* infection, the differentiated gastric cells in GPCs, seem to develop into naïve progenitor cells, which later take on the nature of intestinal progenitor cells. But as expected and in contrast to GPCs, in the two *H. pylori*- infected gastric cancer (MKN45 and AGS) cell lines, less naïve and intestinal progenitor cells and more intestinally differentiated cells become expanded. Thus, depending on the target gene of interest, and its potential therapeutic manipulations, the herein illustrated time course of gene expression, in three different cell lines, following *H. pylori* infection, will allow for an educated choice of cell line and time point, for future study designs.

4. Methods

4.1. Cell culture and tissue specimens

For this study, two gastric primary cells from two different donors[29] and two gastric cancer cell lines (MKN45 and AGS) were used. GPCs were developed as previously described [29]. Briefly, gastric tissues were obtained from *H. pylori*-negative consenting donors, with normal gastric mucosa, under endoscopy at Amiralam Hospital (Tehran, Iran). The tissue specimens were minced, enzymatically digested and used for gastric primary culture on mouse embryonic fibroblast (MEF). GPCs were expanded in advanced DMEM/F12 (Gibco, USA), supplemented with growth factors and small molecules (2-dimensional medium) [29,104]. AGS and MKN45 gastric cancer cell lines were obtained from the Iranian Biological Resource Center (IBRC) cell line collection (Tehran, Iran). Both cell lines were seeded and expanded in DMEM/F12 medium (Gibco, USA), supplemented with 10 mM L-glutamine, 10% (v/v) fetal bovine serum (Gibco, USA) and 1% penicillin/streptomycin and incubated at 37°C in a humidified incubator with 5% CO_2, for the duration of each experiment. All tissue specimens, including those of the gastric tumor, its normal counterpart and duodenum of a GPCs donor, were collected *via* gastroscopy. All experiments and methods were performed in accordance with relevant guidelines and regulations. All experimental protocols were approved by a named institutional/licencing committee. Specifically, human gastric tissue specimens were approved by the Committee on Ethical Issues in Medical Research, Pasteur Institute of Iran (IPI); Ref No. IR.PII.REC.1394.57. (Tehran, Iran). Informed consent was obtained from all subjects,

and all methods were carried out in accordance with the relevant guidelines and regulations of IPI Ethics Committee.

4.2. Bacterial strain culture and characterization

4.2.1. *H. pylori* culture and isolation

An *H. pylori* (C142LD) strain, originally isolated from a gastric cancer patient, was selected for this study. As previously described [105], the C142LD strain was cultured on *H. pylori* Special Peptone Agar (HPSPA) plates, and incubated at 37°C under microaerophilic conditions (10% CO_2, 5% O_2 and 85% N_2), for 7–10 days. The grown strain was confirmed as *H. pylori* by routine microbiological assays, including gram staining, urease, catalase and oxidase tests. Sweeps of grown bacteria were serially subcultured, in order to obtain single colonies.

4.2.2. Genomic DNA extraction and PCR

Whole genomic DNA extraction from C142LD *H. pylori* strain was carried out, using DNA Mini Kit (Qiagen DNeasy Blood & Tissue Kit, Germany), following the manufacturer's recommendations. The extracted DNA was, then, checked for the presence of *glmM, cagA, vacA*, and *babA/B* genes by gene-specific PCRs (Supplementary Table-1).

4.2.3. Protein expression assays

The C142LD strain was evaluated for the expression of CagA, VacA, and BabA proteins, according to the previously published methods [106]. In brief, plates of full-grown bacteria were washed with PBS and centrifuged at 6000 rcf for 5 min, followed by resuspension in 500 µl reduced Laemmli sample buffer (Biorad, USA) and incubated at 100°C for 10 minutes. The samples were then centrifuged at 3000 rcf for 5 minutes. Bacterial lysates (70 µg/strain) were applied on 10% SDS-PAGE and analyzed by silver nitrate staining. Western blotting was performed using 1:1000 dilution of first antibodies (CagA- and VacA-specific polyclonal antibodies, Austral Biologicals, USA) and gift BabA antibody (generously provided by Prof. Thomas Boren, University of Umea, Sweden), all of which were detected by horseradish peroxidase (HRP)-conjugated anti-rabbit antibody (1:5000, Dako, Denmark). Blots were developed by DAB (3,3-diaminobenzidine) solution (Sigma, USA).

4.4. *H. pylori* liquid culture

The C142LD strain was expanded in liquid culture, according to a previously optimized protocol [107]. In brief, a single colony of C142LD strain was grown in Brucella broth (Difco, USA), supplemented with 0.2% β-cyclodextrin (Fluka, USA), under microaerophilic conditions and continuous shaking at 120 rpm, for 24 hours at 37°C. When the turbidity of the bacterial suspension reached an optical density of ~ 1 unit at 550 nm, bacteria were collected by centrifugation (3000 g, for 15 minutes). The viability and possible contamination of the collected bacteria were checked, by wet mount, under light microscopy and cultured onto blood agar plates for 3 days, respectively.

4.5. Co-culture assays

Twenty-four hours prior to *H. pylori* infection, the culture media on GPCs (antibiotic-free 2-dimensional [29,104]), MKN45 and AGS cells (DMEM/F12) were refreshed. On the day of the experiment, the liquid culture-harvested C142LD *H. pylori* was washed with phosphate-buffered saline (PBS), resuspended in each cell-specific growth medium, and diluted to a final concentration of 1×10^8 CFU/mL. The viability of *H. pylori* cells was monitored by DiI (ThermoFisher) live staining, according to manufacturer's instructions. In parallel, the cells (GPCs, MKN45, and AGS) were rinsed with PBS and fresh media were added. Thereafter, the bacterial suspension was added to the cell cultures (in triplicates), at the multiplicity of infection (MOI) of 1:1, for up to 96h. The MOI was determined according to approximate cell counts, which were based on standard curves, using a nontoxic cell counting solution (Orangu™; Cell Guidance System, UK). The cultures of infected and uninfected cells were sampled at 6-time intervals (0, 8, 24, 48, 72, and 96h) post infection.

4.6. Vacuolation and hummingbird assay

The vacuolation and hummingbird assays were performed to determine: 1) the functional activity of the C142LD *H. pylori* strain on AGS cell line and 2) investigation of GPCs, MKN45 and AGS cellular changes up to 96h, following *H. pylori* infection. The morphology of the cells was examined, using an inverted light microscope. Observation of vacuole formation in more than 50% of the cells, in 10 different microscopic fields at ×40 magnification, was defined as a positive vacuolation phenotype [108]. An elongated hummingbird phenotype (the ratio of the most extended protrusion to the shortest protrusion of greater than 2), was also scored in 10 different microscopic fields at ×40 magnification and the average elongation length was measured and documented [109]. *H. pylori*-untreated cells were assessed as negative controls.

4.7. IL-8 secretion

IL-8 secretion by *H. pylori*-infected cells was assessed, at 24h PI, to ensure bacterial-cell interaction. Cell supernatants were centrifuged at 15,000 rcf, for 10 minutes and stored at -80°C, until further use. IL-8 levels were measured using a commercial human IL-8 kit (CytoSet; Invitrogen Corporation, USA and DuoSet ELISA; R&D Systems, Canada), according to manufacturer's instructions. IL-8 concentrations were determined based on a standard curve and recorded as pg/10^6 cells.

4.8. Cell viability

The viability of the co-cultures was ascertained throughout the experiment, using Orangu assay, according to manufacturer instructions. Briefly, an optimum amount (10% of the culture medium) of Orangu solution (OR01-500, Cell Guidance Systems, UK) was added to the co-cultures, at 8 to 96h post treatment. The plates were then incubated at 37°C for 1 hour. The optical density (OD_{450}) of the cell supernatants were quantitated using a microplate reader. The assay was based on the reduction of water-

soluble tetrazolium salt by dehydrogenase, which forms formazan dye in direct proportion with the number of live cells [110].

4.9. RNA extraction and quantitative real-time PCR

Total RNA was extracted from GPCs, MKN45 and AGS cells, as well as tissue specimens of intestinal type gastric tumor, its normal gastric counterpart and the duodenum, using Trizol reagent (Invitrogen, USA). According to the manufacturer's instruction [111], complementary DNA strands (cDNA) were generated using the high-capacity cDNA reverse transcription kit (ABI, USA). Quantitative real-time PCR (qRT-PCR) reactions were performed (in duplicates), using SYBR green (ABI, USA) and gene-specific primers to amplify the target and house-keeping genes (glyceraldehyde-3-phosphate dehydrogenase; GAPDH) (Supplementary Table-2). qRT-PCR reactions were carried out using ABI One-Step 7500 Real-Time system (ABI, USA), at 50°C for 2 min, 95°C for 10 min, followed by 50 cycles at 95°C for 15s, and at 60°C for 1 min. The expression of GAPDH was used to normalize that of the target genes alteration by Qrel ($2^{-\Delta Ct}$) [112] and $2^{-\Delta\Delta Ct}$ methods. Log2 transformed values were used to create more symmetrical and normally distributed data, in order to reduce statistical errors[113].

4.10. Statistical analysis

Gene expression data from quantitative RT-PCR were expressed as mean ± standard deviation (SD) of three independent experiments and analyzed using GraphPad Prism (version 8.0.0 for Mac GraphPad Software, San Diego, California USA, www.graphpad.com). The differences between groups were evaluated by one-way analysis of variance (ANOVA), followed by post hoc contrasts, using the Bonferroni limitation for the statistical analysis. *P* values less than 0.05 were considered as statistically significant. To visualize hierarchical clustering of gene expression, the “Heatmap” package in R was used. Hierarchical clustering was performed in two steps: 1) calculating the distance matrix and apply clustering according to the absolute fold-changes in gene expression and 2) the correlation distance was defined as 1 – cor (x, y, method). The euclidean distance was calculated by “dist()” function [114].

Declarations

Acknowledgement

This study was funded by Pasteur Institute of Iran: Grant/Award Number: #722; and #TP-9121 and Royan Institute: Grant/Award Number: 94000090

Data availability

The datasets generated during and/or analysed during the current study are available from the corresponding author on reasonable request.

Author Contributions Statement

SS and MM conceived the original idea and co-designed the study. SS carried out the experiments, did the analysis and wrote the manuscript. MM helped interpret the results and revised the manuscript. ME carried out patient sampling and laboratory processing. MT collected the gastric specimens. MEH supervised and carried out the gastroscopy and medical diagnosis. HB supported in providing the laboratory facilities. MM supervised the entire project.

Conflict of interest

None declared

References

1. Camilo, V., Sugiyama, T. & Touati, E. Pathogenesis of Helicobacter pylori infection. *Helicobacter* **22 Suppl 1**, doi:10.1111/hel.12405 (2017).
2. Conteduca, V. *et al.* H. pylori infection and gastric cancer: state of the art (review). *Int J Oncol* **42**, 5-18, doi:10.3892/ijo.2012.1701 (2013).
3. Moss, S. F. The Clinical Evidence Linking Helicobacter pylori to Gastric Cancer. *Cell Mol Gastroenterol Hepatol* **3**, 183-191, doi:10.1016/j.jcmgh.2016.12.001 (2017).
4. Bray, F. *et al.* Global cancer statistics 2018: GLOBOCAN estimates of incidence and mortality worldwide for 36 cancers in 185 countries. *CA Cancer J Clin* **68**, 394-424, doi:10.3322/caac.21492 (2018).
5. Correa, P. & Shiao, Y. H. Phenotypic and genotypic events in gastric carcinogenesis. *Cancer Res* **54**, 1941s-1943s (1994).
6. Lauren, P. THE TWO HISTOLOGICAL MAIN TYPES OF GASTRIC CARCINOMA: DIFFUSE AND SO-CALLED INTESTINAL-TYPE CARCINOMA. AN ATTEMPT AT A HISTO-CLINICAL CLASSIFICATION. *Acta Pathol Microbiol Scand* **64**, 31-49, doi:10.1111/apm.1965.64.1.31 (1965).
7. Park, Y. H. & Kim, N. Review of atrophic gastritis and intestinal metaplasia as a premalignant lesion of gastric cancer. *J Cancer Prev* **20**, 25-40, doi:10.15430/jcp.2015.20.1.25 (2015).
8. de Vries, A. C. *et al.* Gastric cancer risk in patients with premalignant gastric lesions: a nationwide cohort study in the Netherlands. *Gastroenterology* **134**, 945-952, doi:10.1053/j.gastro.2008.01.071 (2008).
9. Silva, S. & Filipe, M. I. Intestinal metaplasia and its variants in the gastric mucosa of Portuguese subjects: a comparative analysis of biopsy and gastrectomy material. *Hum Pathol* **17**, 988-995, doi:10.1016/s0046-8177(86)80082-x (1986).
10. Noah, T. K., Donahue, B. & Shroyer, N. F. Intestinal development and differentiation. *Exp Cell Res* **317**, 2702-2710, doi:10.1016/j.yexcr.2011.09.006 (2011).
11. Kim, T. H. & Shivdasani, R. A. Stomach development, stem cells and disease. *Development* **143**, 554-565, doi:10.1242/dev.124891 (2016).

12. Kostouros, A. *et al.* Large intestine embryogenesis: Molecular pathways and related disorders (Review). *Int J Mol Med* **46**, 27-57, doi:10.3892/ijmm.2020.4583 (2020).
13. Rodrigues, J. P. *et al.* Mechanisms of regulation of normal and metaplastic intestinal differentiation. *Histol Histopathol* **33**, 523-532, doi:10.14670/hh-11-938 (2018).
14. Deltenre, M., Jonas, C., Buset, M., Denis, P. & De Koster, E. Gastric carcinoma: the Helicobacter pylori trail. *Acta Gastroenterol Belg* **58**, 193-200 (1995).
15. Molaei, F., Forghanifard, M. M., Fahim, Y. & Abbaszadegan, M. R. Molecular Signaling in Tumorigenesis of Gastric Cancer. *Iran Biomed J* **22**, 217-230, doi:10.22034/ibj.22.4.217 (2018).
16. Ikenoue, T. *et al.* Analysis of the beta-catenin/T cell factor signaling pathway in 36 gastrointestinal and liver cancer cells. *Jpn J Cancer Res* **93**, 1213-1220, doi:10.1111/j.1349-7006.2002.tb01226.x (2002).
17. Ooi, C. H. *et al.* Oncogenic pathway combinations predict clinical prognosis in gastric cancer. *PLoS Genet* **5**, e1000676, doi:10.1371/journal.pgen.1000676 (2009).
18. Clements, W. M. *et al.* beta-Catenin mutation is a frequent cause of Wnt pathway activation in gastric cancer. *Cancer Res* **62**, 3503-3506 (2002).
19. Fafilek, B. *et al.* Troy, a tumor necrosis factor receptor family member, interacts with lgr5 to inhibit wnt signaling in intestinal stem cells. *Gastroenterology* **144**, 381-391, doi:10.1053/j.gastro.2012.10.048 (2013).
20. Song, X., Xin, N., Wang, W. & Zhao, C. Wnt/β-catenin, an oncogenic pathway targeted by H. pylori in gastric carcinogenesis. *Oncotarget* **6**, 35579-35588, doi:10.18632/oncotarget.5758 (2015).
21. Sigal, M. *et al.* Helicobacter pylori Activates and Expands Lgr5(+) Stem Cells Through Direct Colonization of the Gastric Glands. *Gastroenterology* **148**, 1392-1404.e1321, doi:10.1053/j.gastro.2015.02.049 (2015).
22. Tsang, Y. H., Lamb, A. & Chen, L. F. New insights into the inactivation of gastric tumor suppressor RUNX3: the role of H. pylori infection. *J Cell Biochem* **112**, 381-386, doi:10.1002/jcb.22964 (2011).
23. Tang, B. *et al.* A flexible reporter system for direct observation and isolation of cancer stem cells. *Stem Cell Reports* **4**, 155-169, doi:10.1016/j.stemcr.2014.11.002 (2015).
24. Corfield, A. P. Mucins: a biologically relevant glycan barrier in mucosal protection. *Biochim Biophys Acta* **1850**, 236-252, doi:10.1016/j.bbagen.2014.05.003 (2015).
25. Silva, E. *et al.* Mucins as key molecules for the classification of intestinal metaplasia of the stomach. *Virchows Arch* **440**, 311-317, doi:10.1007/s004280100531 (2002).
26. Johansson, M. E. *et al.* Composition and functional role of the mucus layers in the intestine. *Cell Mol Life Sci* **68**, 3635-3641, doi:10.1007/s00018-011-0822-3 (2011).
27. Babu, S. D., Jayanthi, V., Devaraj, N., Reis, C. A. & Devaraj, H. Expression profile of mucins (MUC2, MUC5AC and MUC6) in Helicobacter pylori infected pre-neoplastic and neoplastic human gastric epithelium. *Mol Cancer* **5**, 10, doi:10.1186/1476-4598-5-10 (2006).

28. Douraghi, M., Talebkhan, Y., Zeraati, H. & Mohammadi, M. Cooperative genotyping for Helicobacter pylori virulence determinants strengthens the predictive value of gastric cancer risk assessment. *Dig Liver Dis* **42**, 662-663, doi:10.1016/j.dld.2010.01.010 (2010).
29. Saberi, S. *et al.* A simple and cost-efficient adherent culture platform for human gastric primary cells, as an in vitro model for Helicobacter pylori infection. *Helicobacter* **23**, e12489, doi:10.1111/hel.12489 (2018).
30. Zambon, C. F., Navaglia, F., Basso, D., Rugge, M. & Plebani, M. Helicobacter pylori babA2, cagA, and s1 vacA genes work synergistically in causing intestinal metaplasia. *J Clin Pathol* **56**, 287-291, doi:10.1136/jcp.56.4.287 (2003).
31. Naito, M. *et al.* Influence of EPIYA-repeat polymorphism on the phosphorylation-dependent biological activity of Helicobacter pylori CagA. *Gastroenterology* **130**, 1181-1190, doi:10.1053/j.gastro.2005.12.038 (2006).
32. Saberi, S. *et al.* A potential association between Helicobacter pylori CagA EPIYA and multimerization motifs with cytokeratin 18 cleavage rate during early apoptosis. *Helicobacter* **17**, 350-357, doi:10.1111/j.1523-5378.2012.00954.x (2012).
33. Talebkhan, Y. *et al.* cagA gene and protein status among Iranian Helicobacter pylori strains. *Dig Dis Sci* **53**, 925-932, doi:10.1007/s10620-007-9978-y (2008).
34. Rhead, J. L. *et al.* A new Helicobacter pylori vacuolating cytotoxin determinant, the intermediate region, is associated with gastric cancer. *Gastroenterology* **133**, 926-936, doi:10.1053/j.gastro.2007.06.056 (2007).
35. Bugaytsova, J. A. *et al.* Helicobacter pylori Adapts to Chronic Infection and Gastric Disease via pH-Responsive BabA-Mediated Adherence. *Cell Host Microbe* **21**, 376-389, doi:10.1016/j.chom.2017.02.013 (2017).
36. Saberi, S. *et al.* Helicobacter pylori Strains from Duodenal Ulcer Patients Exhibit Mixed babA/B Genotypes with Low Levels of BabA Adhesin and Lewis b Binding. *Dig Dis Sci* **61**, 2868-2877, doi:10.1007/s10620-016-4217-z (2016).
37. Schwartz, G. K. Invasion and metastases in gastric cancer: in vitro and in vivo models with clinical correlations. *Semin Oncol* **23**, 316-324 (1996).
38. Pompaiah, M. & Bartfeld, S. Gastric Organoids: An Emerging Model System to Study Helicobacter pylori Pathogenesis. *Curr Top Microbiol Immunol* **400**, 149-168, doi:10.1007/978-3-319-50520-6_7 (2017).
39. Yokozaki, H. Molecular characteristics of eight gastric cancer cell lines established in Japan. *Pathol Int* **50**, 767-777, doi:10.1046/j.1440-1827.2000.01117.x (2000).
40. Barranco, S. C. *et al.* Establishment and characterization of an in vitro model system for human adenocarcinoma of the stomach. *Cancer Res* **43**, 1703-1709 (1983).
41. Matsuda, K. *et al.* Quantitative analysis of the effect of Helicobacter pylori on the expressions of SOX2, CDX2, MUC2, MUC5AC, MUC6, TFF1, TFF2, and TFF3 mRNAs in human gastric carcinoma cells. *Scand J Gastroenterol* **43**, 25-33, doi:10.1080/00365520701579795 (2008).

42. Ji, J. *et al.* Comprehensive analysis of the gene expression profiles in human gastric cancer cell lines. *Oncogene* **21**, 6549-6556, doi:10.1038/sj.onc.1205829 (2002).
43. Akama, Y. *et al.* Genetic status and expression of the cyclin-dependent kinase inhibitors in human gastric carcinoma cell lines. *Jpn J Cancer Res* **87**, 824-830, doi:10.1111/j.1349-7006.1996.tb02106.x (1996).
44. Cinghu, S. *et al.* Phosphorylation of the gastric tumor suppressor RUNX3 following H. pylori infection results in its localization to the cytoplasm. *J Cell Physiol* **227**, 1071-1080, doi:10.1002/jcp.22820 (2012).
45. Chiurillo, M. A. Role of the Wnt/β-catenin pathway in gastric cancer: An in-depth literature review. *World J Exp Med* **5**, 84-102, doi:10.5493/wjem.v5.i2.84 (2015).
46. Barker, N. *et al.* Lgr5(+ve) stem cells drive self-renewal in the stomach and build long-lived gastric units in vitro. *Cell Stem Cell* **6**, 25-36, doi:10.1016/j.stem.2009.11.013 (2010).
47. Cai, C. & Zhu, X. The Wnt/β-catenin pathway regulates self-renewal of cancer stem-like cells in human gastric cancer. *Mol Med Rep* **5**, 1191-1196, doi:10.3892/mmr.2012.802 (2012).
48. Kang, J. M. *et al.* CDX1 and CDX2 expression in intestinal metaplasia, dysplasia and gastric cancer. *J Korean Med Sci* **26**, 647-653, doi:10.3346/jkms.2011.26.5.647 (2011).
49. Ito, K. *et al.* RUNX3, a novel tumor suppressor, is frequently inactivated in gastric cancer by protein mislocalization. *Cancer Res* **65**, 7743-7750, doi:10.1158/0008-5472.Can-05-0743 (2005).
50. Ito, K. *et al.* RUNX3 attenuates beta-catenin/T cell factors in intestinal tumorigenesis. *Cancer Cell* **14**, 226-237, doi:10.1016/j.ccr.2008.08.004 (2008).
51. Bahnassy, A. A. *et al.* The role of E-cadherin and Runx3 in Helicobacter Pylori - Associated gastric carcinoma is achieved through regulating P21waf and P27 expression. *Cancer Genet* **228-229**, 64-72, doi:10.1016/j.cancergen.2018.08.006 (2018).
52. Maekita, T. *et al.* High levels of aberrant DNA methylation in Helicobacter pylori-infected gastric mucosae and its possible association with gastric cancer risk. *Clin Cancer Res* **12**, 989-995, doi:10.1158/1078-0432.Ccr-05-2096 (2006).
53. Fan, X. Y. *et al.* Association between RUNX3 promoter methylation and gastric cancer: a meta-analysis. *BMC Gastroenterol* **11**, 92, doi:10.1186/1471-230x-11-92 (2011).
54. Liu, X., Wang, L. & Guo, Y. The association between runt-related transcription factor 3 gene promoter methylation and gastric cancer: A meta-analysis. *J Cancer Res Ther* **12**, 50-53, doi:10.4103/0973-1482.191630 (2016).
55. Xia, Y., Zhang, M., Zhang, X. & Liu, X. A systematic review and meta-analysis of runt-related transcription factor 3 gene promoter hypermethylation and risk of gastric cancer. *J Cancer Res Ther* **10 Suppl**, 310-313, doi:10.4103/0973-1482.151539 (2014).
56. Liu, B. *et al.* Clinicopathological and prognostic significance of the RUNX3 expression in gastric cancer: a systematic review and meta-analysis. *Int J Surg* **53**, 122-128, doi:10.1016/j.ijsu.2018.03.041 (2018).

57. Katayama, Y., Takahashi, M. & Kuwayama, H. Helicobacter pylori causes runx3 gene methylation and its loss of expression in gastric epithelial cells, which is mediated by nitric oxide produced by macrophages. *Biochem Biophys Res Commun* **388**, 496-500, doi:10.1016/j.bbrc.2009.08.003 (2009).
58. Voon, D. C. *et al.* Runx3 protects gastric epithelial cells against epithelial-mesenchymal transition-induced cellular plasticity and tumorigenicity. *Stem Cells* **30**, 2088-2099, doi:10.1002/stem.1183 (2012).
59. Que, J. *et al.* Multiple dose-dependent roles for Sox2 in the patterning and differentiation of anterior foregut endoderm. *Development* **134**, 2521-2531, doi:10.1242/dev.003855 (2007).
60. Arnold, K. *et al.* Sox2(+) adult stem and progenitor cells are important for tissue regeneration and survival of mice. *Cell Stem Cell* **9**, 317-329, doi:10.1016/j.stem.2011.09.001 (2011).
61. Mutoh, H., Sashikawa, M. & Sugano, K. Sox2 expression is maintained while gastric phenotype is completely lost in Cdx2-induced intestinal metaplastic mucosa. *Differentiation* **81**, 92-98, doi:10.1016/j.diff.2010.10.002 (2011).
62. Li, X. L. *et al.* Expression of the SRY-related HMG box protein SOX2 in human gastric carcinoma. *Int J Oncol* **24**, 257-263 (2004).
63. Camilo, V. *et al.* Immunohistochemical molecular phenotypes of gastric cancer based on SOX2 and CDX2 predict patient outcome. *BMC Cancer* **14**, 753, doi:10.1186/1471-2407-14-753 (2014).
64. Matsuoka, J. *et al.* Role of the stemness factors sox2, oct3/4, and nanog in gastric carcinoma. *J Surg Res* **174**, 130-135, doi:10.1016/j.jss.2010.11.903 (2012).
65. Wang, S. *et al.* SOX2, a predictor of survival in gastric cancer, inhibits cell proliferation and metastasis by regulating PTEN. *Cancer Lett* **358**, 210-219, doi:10.1016/j.canlet.2014.12.045 (2015).
66. Otsubo, T., Akiyama, Y., Yanagihara, K. & Yuasa, Y. SOX2 is frequently downregulated in gastric cancers and inhibits cell growth through cell-cycle arrest and apoptosis. *Br J Cancer* **98**, 824-831, doi:10.1038/sj.bjc.6604193 (2008).
67. Du, X. M. *et al.* Prognostic value of Sox2 expression in digestive tract cancers: A meta-analysis. *J Huazhong Univ Sci Technolog Med Sci* **36**, 305-312, doi:10.1007/s11596-016-1584-9 (2016).
68. Hütz, K. *et al.* The stem cell factor SOX2 regulates the tumorigenic potential in human gastric cancer cells. *Carcinogenesis* **35**, 942-950, doi:10.1093/carcin/bgt410 (2014).
69. Yuan, X. *et al.* SALL4 promotes gastric cancer progression through activating CD44 expression. *Oncogenesis* **5**, e268, doi:10.1038/oncsis.2016.69 (2016).
70. Chia, N. Y. *et al.* Regulatory crosstalk between lineage-survival oncogenes KLF5, GATA4 and GATA6 cooperatively promotes gastric cancer development. *Gut* **64**, 707-719, doi:10.1136/gutjnl-2013-306596 (2015).
71. He, J. *et al.* Inhibition of SALL4 reduces tumorigenicity involving epithelial-mesenchymal transition via Wnt/β-catenin pathway in esophageal squamous cell carcinoma. *J Exp Clin Cancer Res* **35**, 98, doi:10.1186/s13046-016-0378-z (2016).

72. Zhang, D., Jiang, F., Wang, X. & Li, G. Knockdown of SALL4 Inhibits Proliferation, Migration, and Invasion in Osteosarcoma Cells. *Oncol Res* **25**, 763-771, doi:10.3727/096504016x14772402056137 (2017).
73. Ma, Y. *et al.* SALL4, a novel oncogene, is constitutively expressed in human acute myeloid leukemia (AML) and induces AML in transgenic mice. *Blood* **108**, 2726-2735, doi:10.1182/blood-2006-02-001594 (2006).
74. Liu, J., Wang, L., Yang, A., Jiang, P. & Wang, M. Up-regulation of SALL4 associated with poor prognosis in gastric cancer. *Hepatogastroenterology* **61**, 1459-1464 (2014).
75. Miettinen, M. *et al.* SALL4 expression in germ cell and non-germ cell tumors: a systematic immunohistochemical study of 3215 cases. *Am J Surg Pathol* **38**, 410-420, doi:10.1097/pas.0000000000000116 (2014).
76. Noto, J. M. *et al.* Helicobacter pylori promotes the expression of Krüppel-like factor 5, a mediator of carcinogenesis, in vitro and in vivo. *PLoS One* **8**, e54344, doi:10.1371/journal.pone.0054344 (2013).
77. Nakaya, T. *et al.* KLF5 regulates the integrity and oncogenicity of intestinal stem cells. *Cancer Res* **74**, 2882-2891, doi:10.1158/0008-5472.Can-13-2574 (2014).
78. Liu, J. *et al.* Spheroid body-forming cells in the human gastric cancer cell line MKN-45 possess cancer stem cell properties. *Int J Oncol* **42**, 453-459, doi:10.3892/ijo.2012.1720 (2013).
79. Zhang, C., Li, C., He, F., Cai, Y. & Yang, H. Identification of CD44+CD24+ gastric cancer stem cells. *J Cancer Res Clin Oncol* **137**, 1679-1686, doi:10.1007/s00432-011-1038-5 (2011).
80. Saberi, S. *et al.* Immunohistochemical Analysis of LGR5 and TROY Expression in Gastric Carcinogenesis Demonstrates an Inverse Trend. *Iran Biomed J* **23**, 107-120, doi:10.29252/.23.2.107 (2019).
81. Wilhelm, F., Böger, C., Krüger, S., Behrens, H. M. & Röcken, C. Troy is expressed in human stomach mucosa and a novel putative prognostic marker of intestinal type gastric cancer. *Oncotarget* **8**, 50557-50569, doi:10.18632/oncotarget.10672 (2017).
82. Zheng, Z. X. *et al.* Intestinal stem cell marker LGR5 expression during gastric carcinogenesis. *World J Gastroenterol* **19**, 8714-8721, doi:10.3748/wjg.v19.i46.8714 (2013).
83. Muñoz, J. *et al.* The Lgr5 intestinal stem cell signature: robust expression of proposed quiescent '+4' cell markers. *Embo j* **31**, 3079-3091, doi:10.1038/emboj.2012.166 (2012).
84. Craig, S. W. & Powell, L. D. Regulation of actin polymerization by villin, a 95,000 dalton cytoskeletal component of intestinal brush borders. *Cell* **22**, 739-746, doi:10.1016/0092-8674(80)90550-4 (1980).
85. Qiao, X. T. *et al.* Prospective identification of a multilineage progenitor in murine stomach epithelium. *Gastroenterology* **133**, 1989-1998, doi:10.1053/j.gastro.2007.09.031 (2007).
86. Guo, R. J., Suh, E. R. & Lynch, J. P. The role of Cdx proteins in intestinal development and cancer. *Cancer Biol Ther* **3**, 593-601, doi:10.4161/cbt.3.7.913 (2004).
87. Grainger, S., Savory, J. G. & Lohnes, D. Cdx2 regulates patterning of the intestinal epithelium. *Dev Biol* **339**, 155-165, doi:10.1016/j.ydbio.2009.12.025 (2010).

88. Silberg, D. G., Swain, G. P., Suh, E. R. & Traber, P. G. Cdx1 and cdx2 expression during intestinal development. *Gastroenterology* **119**, 961-971, doi:10.1053/gast.2000.18142 (2000).
89. Silberg, D. G. *et al.* CDX1 protein expression in normal, metaplastic, and neoplastic human alimentary tract epithelium. *Gastroenterology* **113**, 478-486, doi:10.1053/gast.1997.v113.pm9247467 (1997).
90. Lickert, H. *et al.* Wnt/(beta)-catenin signaling regulates the expression of the homeobox gene Cdx1 in embryonic intestine. *Development* **127**, 3805-3813 (2000).
91. Yu, J. *et al.* CDX2 inhibits the proliferation and tumor formation of colon cancer cells by suppressing Wnt/β-catenin signaling via transactivation of GSK-3β and Axin2 expression. *Cell Death Dis* **10**, 26, doi:10.1038/s41419-018-1263-9 (2019).
92. Choi, S. I. *et al.* CDX1 Expression Induced by CagA-Expressing Helicobacter pylori Promotes Gastric Tumorigenesis. *Mol Cancer Res* **17**, 2169-2183, doi:10.1158/1541-7786.Mcr-19-0181 (2019).
93. Jin, H. F., Dai, J. F., Meng, L. N. & Lu, B. Curcuma wenyujin Y. H. Chen et C. Ling n-Butyl Alcohol Extract Inhibits AGS Cell Helicobacter pylori(CagA+VacA+) Promoted Invasiveness by Down-Regulating Caudal Type Homeobox Transcription Factor and Claudin-2 Expression. *Chin J Integr Med* **26**, 122-129, doi:10.1007/s11655-017-2958-y (2020).
94. Van de Bovenkamp, J. H. *et al.* The MUC5AC glycoprotein is the primary receptor for Helicobacter pylori in the human stomach. *Helicobacter* **8**, 521-532, doi:10.1046/j.1523-5378.2003.00173.x (2003).
95. Hayashi, T. *et al.* Tertiary structure-function analysis reveals the pathogenic signaling potentiation mechanism of Helicobacter pylori oncogenic effector CagA. *Cell Host Microbe* **12**, 20-33, doi:10.1016/j.chom.2012.05.010 (2012).
96. Shi, D., Liu, Y., Wu, D. & Hu, X. Transfection of the Helicobacter pylori CagA gene alters MUC5AC expression in human gastric cancer cells. *Oncol Lett* **15**, 5208-5212, doi:10.3892/ol.2018.7960 (2018).
97. Niv, Y. Helicobacter pylori and gastric mucin expression: A systematic review and meta-analysis. *World J Gastroenterol* **21**, 9430-9436, doi:10.3748/wjg.v21.i31.9430 (2015).
98. Shi, D., Qiu, X. M. & Yan, X. J. The changes in MUC5AC expression in gastric cancer before and after Helicobacter pylori eradication. *Clin Res Hepatol Gastroenterol* **38**, 235-240, doi:10.1016/j.clinre.2013.06.008 (2014).
99. Kang, H. M. *et al.* Effects of Helicobacter pylori Infection on gastric mucin expression. *J Clin Gastroenterol* **42**, 29-35, doi:10.1097/MCG.0b013e3180653cb7 (2008).
100. Ho, S. B. *et al.* Heterogeneity of mucin gene expression in normal and neoplastic tissues. *Cancer Res* **53**, 641-651 (1993).
101. Mejías-Luque, R. *et al.* Inflammation modulates the expression of the intestinal mucins MUC2 and MUC4 in gastric tumors. *Oncogene* **29**, 1753-1762, doi:10.1038/onc.2009.467 (2010).
102. Craanen, M. E., Blok, P., Dekker, W., Ferwerda, J. & Tytgat, G. N. Subtypes of intestinal metaplasia and Helicobacter pylori. *Gut* **33**, 597-600, doi:10.1136/gut.33.5.597 (1992).

103. Reis, C. A. *et al.* Intestinal metaplasia of human stomach displays distinct patterns of mucin (MUC1, MUC2, MUC5AC, and MUC6) expression. *Cancer Res* **59**, 1003-1007 (1999).
104. Schlaermann, P. *et al.* A novel human gastric primary cell culture system for modelling Helicobacter pylori infection in vitro. *Gut* **65**, 202-213, doi:10.1136/gutjnl-2014-307949 (2016).
105. Mohammadi, M., Kashani, S. S., Garoosi, Y. T. & Tazehkand, S. J. In vivo measurement of Helicobacter pylori infection. *Methods Mol Biol* **921**, 239-256, doi:10.1007/978-1-62703-005-2_26 (2012).
106. Karlsson, J. O., Ostwald, K., Kåbjörn, C. & Andersson, M. A method for protein assay in Laemmli buffer. *Anal Biochem* **219**, 144-146, doi:10.1006/abio.1994.1243 (1994).
107. Douraghi, M. *et al.* Comparative evaluation of three supplements for Helicobacter pylori growth in liquid culture. *Curr Microbiol* **60**, 254-262, doi:10.1007/s00284-009-9534-4 (2010).
108. Cover, T. L., Puryear, W., Perez-Perez, G. I. & Blaser, M. J. Effect of urease on HeLa cell vacuolation induced by Helicobacter pylori cytotoxin. *Infect Immun* **59**, 1264-1270, doi:10.1128/iai.59.4.1264-1270.1991 (1991).
109. Chang, C. C. *et al.* Fragmentation of CagA Reduces Hummingbird Phenotype Induction by Helicobactor pylori. *PLoS One* **11**, e0150061, doi:10.1371/journal.pone.0150061 (2016).
110. Lutter, A. H., Scholka, J., Richter, H. & Anderer, U. Applying XTT, WST-1, and WST-8 to human chondrocytes: A comparison of membrane-impermeable tetrazolium salts in 2D and 3D cultures. *Clin Hemorheol Microcirc* **67**, 327-342, doi:10.3233/ch-179213 (2017).
111. Chomczynski, P. A reagent for the single-step simultaneous isolation of RNA, DNA and proteins from cell and tissue samples. *Biotechniques* **15**, 532-534, 536-537 (1993).
112. Livak, K. J. & Schmittgen, T. D. Analysis of relative gene expression data using real-time quantitative PCR and the 2(-Delta Delta C(T)) Method. *Methods* **25**, 402-408, doi:10.1006/meth.2001.1262 (2001).
113. Qin, S., Kim, J., Arafat, D. & Gibson, G. Effect of normalization on statistical and biological interpretation of gene expression profiles. *Front Genet* **3**, 160, doi:10.3389/fgene.2012.00160 (2012).
114. Zhang, Z., Murtagh, F., Van Poucke, S., Lin, S. & Lan, P. Hierarchical cluster analysis in clinical research with heterogeneous study population: highlighting its visualization with R. *Ann Transl Med* **5**, 75, doi:10.21037/atm.2017.02.05 (2017).
115. Labigne, A., Cussac, V. & Courcoux, P. Shuttle cloning and nucleotide sequences of Helicobacter pylori genes responsible for urease activity. *J Bacteriol* **173**, 1920-1931, doi:10.1128/jb.173.6.1920-1931.1991 (1991).
116. Atherton, J. C. *et al.* Mosaicism in vacuolating cytotoxin alleles of Helicobacter pylori. Association of specific vacA types with cytotoxin production and peptic ulceration. *J Biol Chem* **270**, 17771-17777, doi:10.1074/jbc.270.30.17771 (1995).
117. Yamaoka, Y. *et al.* Relationship between Helicobacter pylori iceA, cagA, and vacA status and clinical outcome: studies in four different countries. *J Clin Microbiol* **37**, 2274-2279 (1999).

118. Rudi, J. *et al.* Diversity of Helicobacter pylori vacA and cagA genes and relationship to VacA and CagA protein expression, cytotoxin production, and associated diseases. *J Clin Microbiol* **36**, 944-948 (1998).

119. Colbeck, J. C., Hansen, L. M., Fong, J. M. & Solnick, J. V. Genotypic profile of the outer membrane proteins BabA and BabB in clinical isolates of Helicobacter pylori. *Infect Immun* **74**, 4375-4378, doi:10.1128/iai.00485-06 (2006).

120. Fujii, Y. *et al.* CDX1 confers intestinal phenotype on gastric epithelial cells via induction of stemness-associated reprogramming factors SALL4 and KLF5. *Proc Natl Acad Sci U S A* **109**, 20584-20589, doi:10.1073/pnas.1208651109 (2012).

121. Voronov, D. *et al.* Transcription factors Runx1 to 3 are expressed in the lacrimal gland epithelium and are involved in regulation of gland morphogenesis and regeneration. *Invest Ophthalmol Vis Sci* **54**, 3115-3125, doi:10.1167/iovs.13-11791 (2013).

122. Yin, X. *et al.* The clinical and prognostic implications of pluripotent stem cell gene expression in hepatocellular carcinoma. *Oncol Lett* **5**, 1155-1162, doi:10.3892/ol.2013.1151 (2013).

123. Saulnier, N. *et al.* Mesenchymal stromal cells multipotency and plasticity: induction toward the hepatic lineage. *Eur Rev Med Pharmacol Sci* **13 Suppl 1**, 71-78 (2009).

Figures

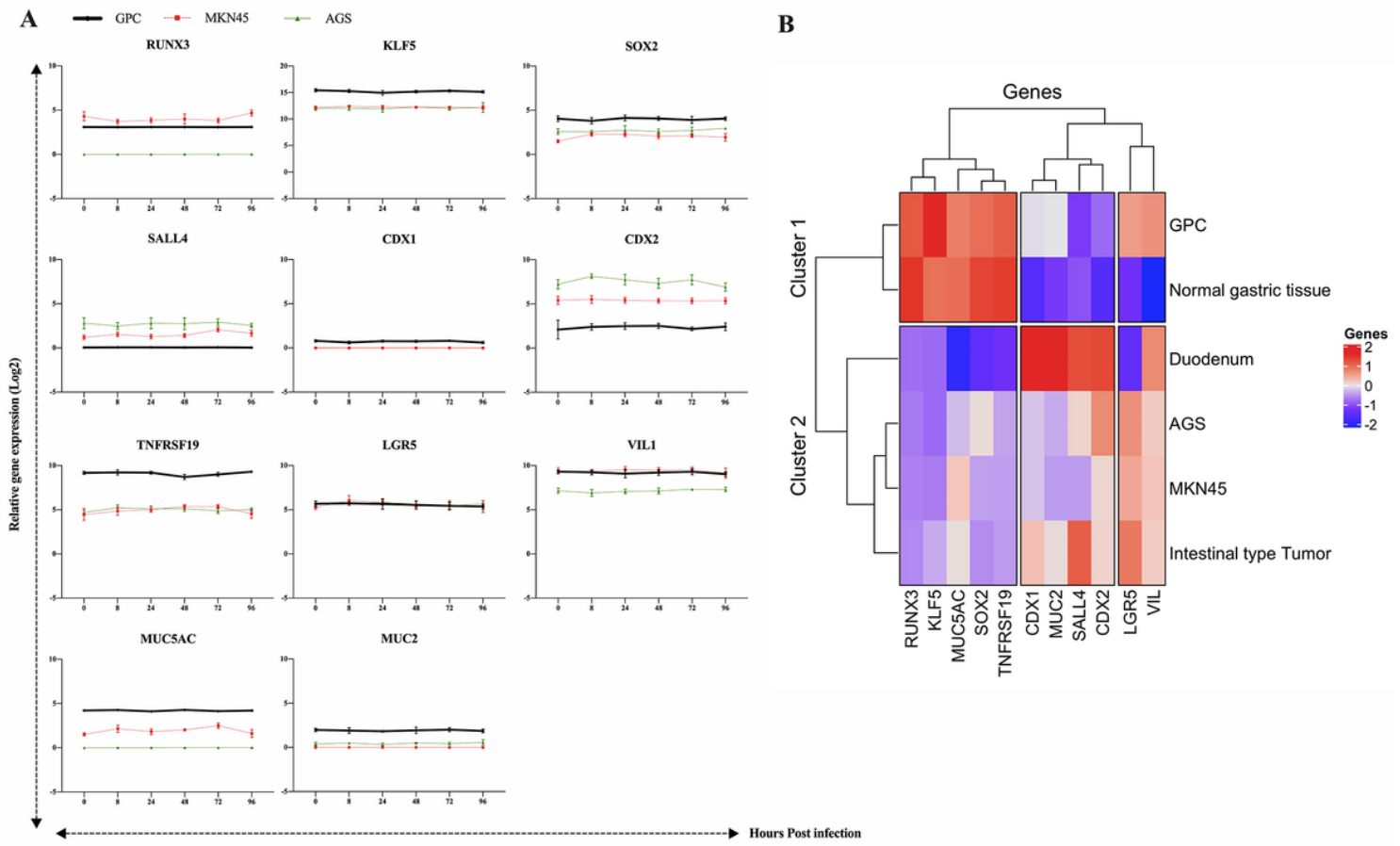

Figure 1

A) Baseline gene expression levels of tissue-specific transcription factors (RUNX3, KLF5, SOX2, SALL4, CDX1, CDX2), Stemness factors (TNFRSF19, LGR5, VIL1) and tissue-specific mucins (MUC5AC, MUC2) in the GPCs, MKN45 and AGS cells from 0 to 96 hours. B) Hierarchical clustering of genes and samples produced by Heatmap function in R, the color-coding scale denotes upregulation in red and downregulation in blue. The expression of GAPDH was used to normalize that of the target genes alteration by Qrel (2−ΔCt) method. Data are expressed as Log2 mean values ± SD (nGPC=4, nMKN45=6 and nAGS=6).

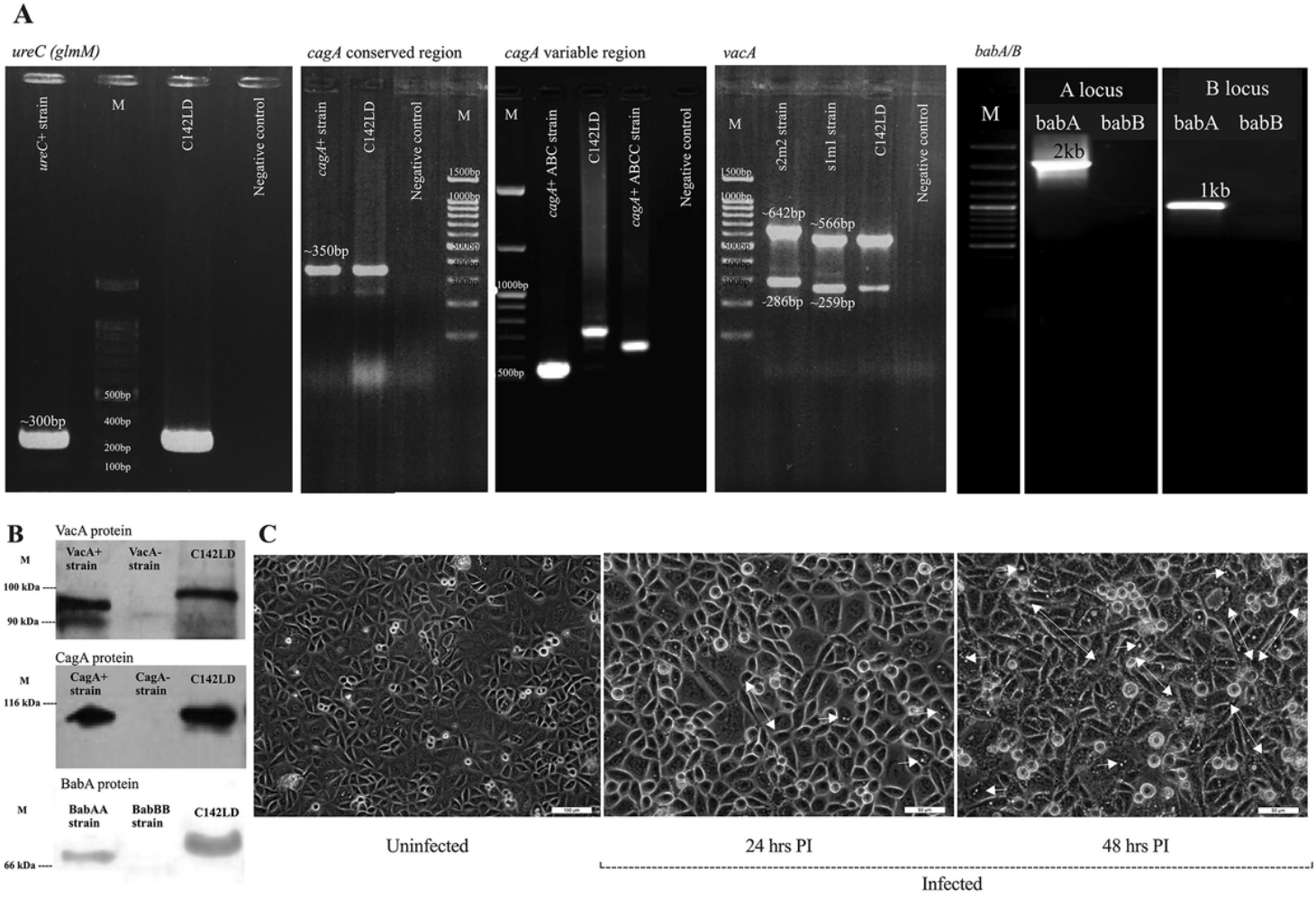

Figure 2

Characterization of H. pylori hypervirulent strain (C142LD). A) PCR results of glmM, cagA (conserved and variable regions), vacA (s and m regions) and babA/B (in A and B loci). B) Western blotting on CagA, VacA and BabA proteins, C) Functional assay on AGS cell line at 24hrs and 48hrs post H. pylori infection (PI), as compared to uninfected cells. Two headed arrows: cell elongation, one headed arrow: vacuoles.

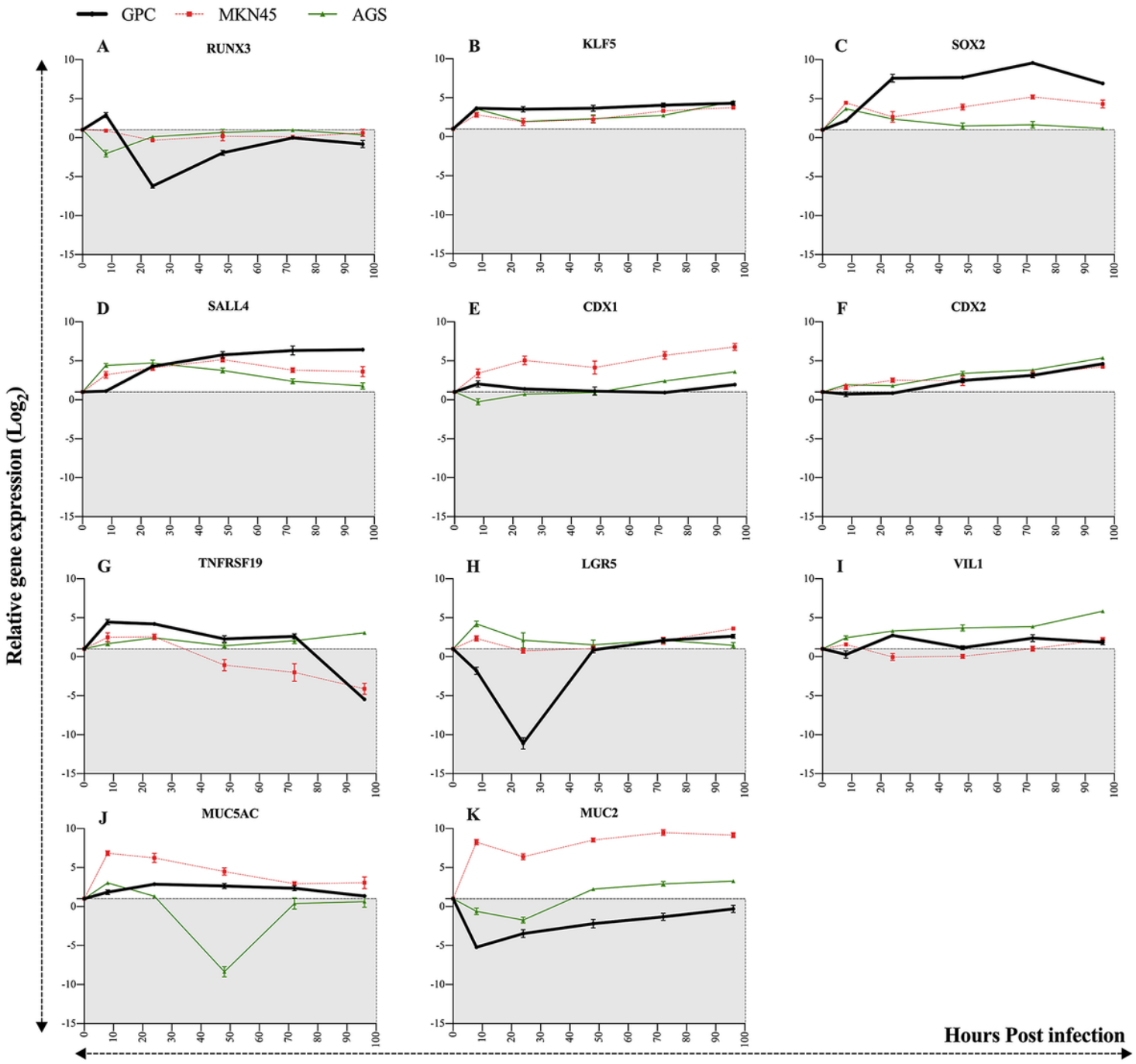

Figure 3

Expression of tissue-specific transcription factors (RUNX3, KLF5, SOX2, SALL4, CDX1, CDX2), Stemness factors (TNFRSF19, LGR5, VIL1) and tissue-specific mucins (MUC5AC, MUC2) in the GPCs, MKN45 and AGS during the course of H. pylori infection (0-96 hrs). The expression of GAPDH was used to normalize that of the target genes alteration by 2−ΔΔCt method. Data are expressed as Log2 mean values ± SD (nGPC=4, nMKN45=6 and nAGS=6).

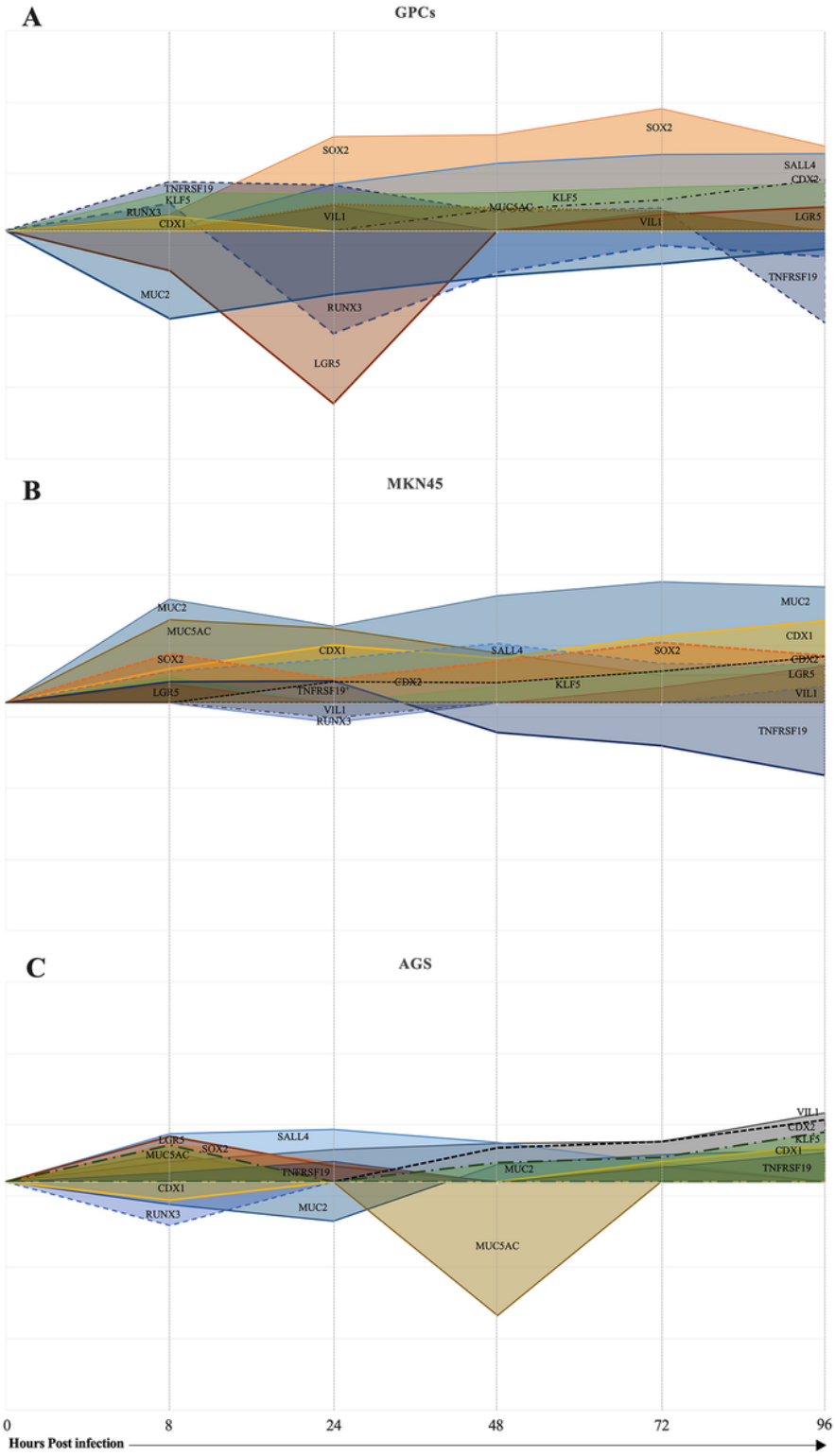

Figure 4

A schematic collective diagram of tissue-specific transcription factors (RUNX3, KLF5, SOX2, SALL4, CDX1, CDX2), Stemness factors (TNFRSF19, LGR5, VIL1) and tissue-specific mucins (MUC5AC, MUC2) expressions in A) GPCs, B) MKN45 and C) AGS, during the time course of H. pylori infection.

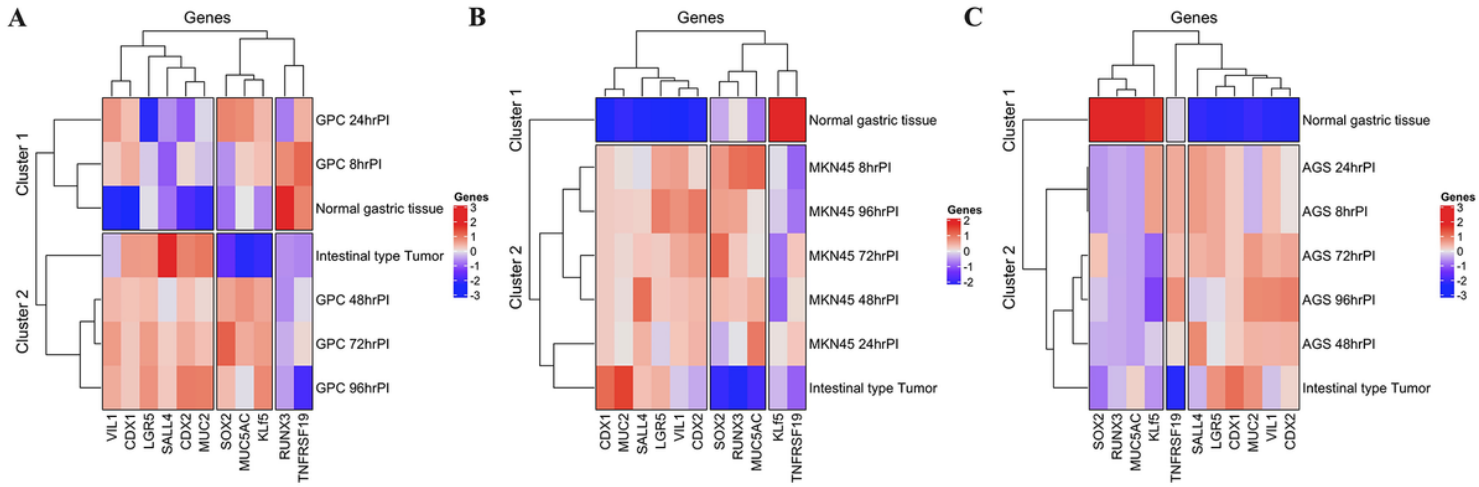

Figure 5

Hierarchical clustering of A) GPCs, B) MKN45 and C) AGS genes expression profiles, after H. pylori infection, as compared normal gastric tissue and intestinal type tumor. This map was produced by Heatmap function in R, the color-coding scale denotes up regulation in red and down regulation in blue. The expression of GAPDH was used to normalize that of the target genes alteration by Qrel (2−ΔCt) method. Data are expressed as Log2 mean values ± SD (nGPC=4, nMKN45=6 and nAGS=6).

Supplementary Files

This is a list of supplementary files associated with this preprint. Click to download.

- SaberietalSupplementaryFigures.pdf
- SaberietalSupplementaryTables.pdf